Screening ion-channel ligand interactions with passive pumping in a microfluidic bilayer lipid membrane chip

Shimul C. Saha,[1,a)] Andrew M. Powl,[2] B. A. Wallace,[2]
Maurits R. R. de Planque,[1] and Hywel Morgan[1,b)]
[1]*Electronics and Computer Science and Institute for Life Sciences, University of Southampton, Southampton SO17 1BJ, United Kingdom*
[2]*Institute of Structural and Molecular Biology, Birkbeck College, University of London, London WC1E 7HX, United Kingdom*

(Received 16 August 2014; accepted 19 December 2014; published online 9 January 2015)

We describe a scalable artificial bilayer lipid membrane platform for rapid electrophysiological screening of ion channels and transporters. A passive pumping method is used to flow microliter volumes of ligand solution across a suspended bilayer within a microfluidic chip. Bilayers are stable at flow rates up to ~0.5 μl/min. Phospholipid bilayers are formed across a photolithographically defined aperture made in a dry film resist within the microfluidic chip. Bilayers are stable for many days and the low shunt capacitance of the thin film support gives low-noise high-quality single ion channel recording. Dose-dependent transient blocking of α-hemolysin with β-cyclodextrin (β-CD) and polyethylene glycol is demonstrated and dose-dependent blocking studies of the KcsA potassium channel with tetraethylammonium show the potential for determining IC_{50} values. The assays are fast (30 min for a complete IC_{50} curve) and simple and require very small amounts of compounds (100 μg in 15 μl). The technology can be scaled so that multiple bilayers can be addressed, providing a screening platform for ion channels, transporters, and nanopores. © *2015 AIP Publishing LLC*.
[http://dx.doi.org/10.1063/1.4905313]

I. INTRODUCTION

Ion channel proteins are present in all biological cell membranes and play an important role in physiological processes, with abnormal channel activity contributing to a wide range of diseases.[1–5] As important drug targets, ion channels are of considerable interest to the pharmaceutical industry.[6] Classical electrophysiology measurements can provide detailed information about the structure-function relationship of ion channels and their modulation by pharmaceutical drugs.

Planar bilayer lipids are now widely used for single ion channel electrophysiology. Parallel recording techniques from multiple bilayers are being pursued[7,8] and improvements in bilayer stability and the ease of bilayer formation have been demonstrated, for example, through the use of smaller apertures over micro-cavities and nanopores.[9–12] Although small apertures are preferable for stable bilayers, the smaller integrated Ag/AgCl electrode can restrict recording time to a few hours.[9,12] Furthermore, the probability of ion-channel incorporation into bilayers is proportional to the surface area,[13] therefore large-area bilayers are desirable but these are often unstable. Stable large-area bilayers have been produced using tapered apertures of 20–30 μm diameter made from Si_3N_4 septa of 240 nm thickness[14] but silicon-based materials introduce undesirable noise. However, shaped apertures can also be fabricated, one at the time, in the negative photoresist SU8 using two-photon direct write lithography.[15]

[a)]Current affiliation: Medical Wireless Sensing Ltd., 42 New Road, E1 2AX, London, UK.
[b)]Author to whom correspondence should be addressed. Electronic mail: hm@ecs.soton.ac.uk.

Many authors have created bilayers across micro-cavities but because of the closed-compartment design, these techniques do not allow access to both sides of the bilayer,[9–11] precluding electrophysiological measurements with asymmetric buffer solutions. Such conditions are often required for ion channel measurements, for example, electrophysiological characterization of the potassium channel KcsA requires an acidic pH on one side of the bilayer.[16,17] In a traditional macro-scale bilayer membrane system,[7,8,17,18] the bilayer is produced across an aperture in a thin hydrophobic material, typically Teflon, separating two cups, providing access to both sides of the bilayer. However, the bilayers are mechanically fragile, and solution exchange is problematic. Furthermore, large volumes (ml) of electrophysiology buffer are required. This issue has been addressed by making smaller systems, incorporating micro-channels for solution exchange.[8,17,19–22] For example, Stimberg *et al*. described a flow channel, where the microfluidic channel and bilayer aperture are made separately and glued together and fluid is flown across the bilayer using a syringe pump.[19] Shao *et al*. demonstrated a bilayer microfluidic platform that enabled rapid perfusion of liquid ($>2.5\,\mu$l/min), with 100 μl samples,[21] and Le Pioufle *et al*. demonstrated an array of wells, each with multiple small bilayers with fluidic access to both sides, where electrical recordings were performed by moving an Ag/AgCl electrode from well to well.[13] Bilayers can also be formed with sessile or falling droplets-in-oil, and flow channels have been integrated into these systems for solution exchange from one side of the bilayer.[23,24] High-volume flow has been demonstrated with such platforms.[23] Tsuji *et al*. described a droplet-interface bilayer system made using two droplets with microchannel perfusion of one droplet.[20] However, all the platforms described above require a syringe pump and a relatively large volume of electrophysiology buffer, and hence a relatively large amount of the compounds that potentially modulate channel activity.

In this paper, we demonstrate a novel scalable bilayer lipid membrane (BLM) system based on micro-fluidic chips. Bilayers are formed across apertures between 50 and 100 μm in diameter that are micro-fabricated in a thin laminate foil. These aperture-suspended bilayers are mechanically stable with a lifetime of many days. Sample flow along the bilayer is realized by passive pumping from small droplets, where the flow is driven by the difference in Laplace pressure between two droplets at either end of a microfluidic channel.[25,26] For microfluidic channels of dimensions $55 \times 100\,\mu$m, the flow rate is up to 0.5 μl/min, with μl volume droplets. This design eliminates the need for syringe pumps and tubing, providing a simple and scalable approach for the delivery of compounds to the bilayers. The platform is compact and is amenable to parallelization with a small footprint, giving a simple automatable system that could be used for high throughput screening of ion channels, transporters, and nanopores with small amounts of effector compounds. We demonstrate the utility of the technology through blocking of α-haemolysin with β-cyclodextrin (β-CD) and polyethylene glycol (PEG). Rapid determination of IC_{50} curves is shown for dose-dependent interaction of the potassium channel KcsA with tetraethylammonium (TEA) demonstrating the ability to examine ion channel behaviour in asymmetric environments (pH).

II. MATERIALS AND METHODS

A. Device design and fabrication

A small (15×15 mm), disposable glass chip contains the fluidics and micro-aperture as shown in Fig. 1. These chips interface with a master board that contains discrete amplifiers for current recording.[27] The chip is made using laminated dry film resist to define both the aperture and the flow channel (Figs. 1(a) and 1(b)). Fig. 1(d) shows a cross section of the chip showing the flow channel and two Ag/AgCl electrodes. Fig. 1(e) is a photograph of a device with the PMMA well that holds the buffer above the bilayer. BLMs are made by painting a lipid-solvent solution across the aperture. The *trans* side of the membrane is accessed via the microfluidic channel, while buffer on the *cis* side is retained within a plastic reservoir of 200 μl volume. Electrical recordings are made using discrete integrated Ag/AgCl electrodes. Each glass chip can hold up to four bilayers, each of which is recorded in parallel,[27] but in this work we use a single aperture. Compared with traditional BLM electrophysiology systems,[11,28,29] both the

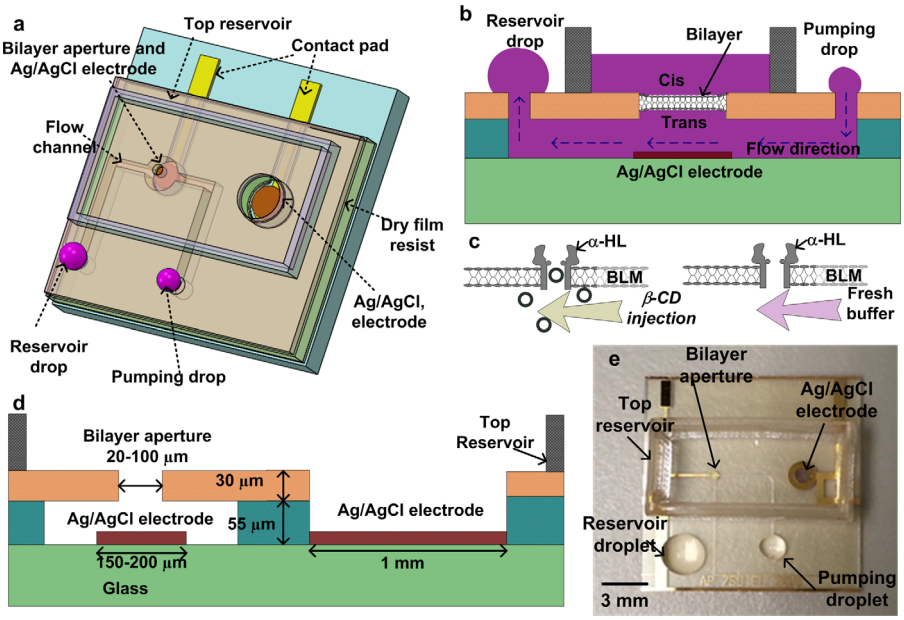

FIG. 1. Illustration of the droplet flow BLM chip. (a) 3-D schematic diagram of the chip with a single bilayer aperture, showing the integrated Ag/AgCl electrodes (one common and one beneath the BLM) and the pumping droplets. (b) Illustration of the micro well and integrated Ag/AgCl electrode showing the direction of fluid flow which is from the small droplet to the large droplet. Note that for ease of illustration, the architecture does not correspond exactly to Fig. 1(a). (c) Diagram demonstrating transient blocking of α-hemolysin by β-cyclodextrin (β-CD) flowing along the *trans* side of the bilayer. (d) Cross section of chip showing the bilayer aperture and electrode. The flow channel is 55 μm high and 100 μm wide. (e) A fabricated chip showing the pumping and reservoir droplet. Also shown is the plastic compartment that defines the top reservoir. Note that (a)–(d) are not to scale.

bilayer and the shunt capacitance are reduced, enabling higher bandwidth low-noise electrical recordings.

Details of the microfluidic chip fabrication have been described previously[27] (detailed in the supplementary material Fig. S1 (Ref. 30)). A four mask process was used. The substrate consisted of a 100 mm diameter 700 μm thick glass wafer. Electrodes and contact pads were made from a 200 nm thick Au layer, defined using photolithography and wet etching. The second mask defines the Ag/AgCl electrodes. The Ag electrodes were plated for ~6 min with a current density of ~2 mA/cm^2 to give a thickness of around 5–6 μm, and were subsequently chlorinated by immersion in $FeCl_3$ solution for 2 min.[31] The first dry film resist layer (TMMF S2055 from Tokyo Okha Koygo Co.) was then laminated to define the micro-well and the microfluidic channel. A second layer of TMMF S2030 was laminated over the first layer at 45 °C to define the BLM aperture.[32] To make the surface hydrophobic (for stable bilayers and control of droplet surface tension), the chips were exposed to a CF_4 plasma, at a gas ratio of 2% O_2 and 98% CF_4, 50 W and 50 mTorr pressure for 2 min. The contact angle for water on the treated TMMF surface was around 115°. A hydrophobic surface also ensures that the aqueous pumping droplets do not spread. Chips could be re-used after washing with water and isopropyl alcohol. After several experiments, the contact angle slowly reduced but chips could be made hydrophobic again by re-exposure to CF_4 plasma. The final device is shown in Fig. 1(e) and is 15×15 mm in size. A poly(methyl methacrylate) (PMMA) chamber of dimension $10 \times 4 \times 5$ mm is glued to the top face to form the *cis* reservoir.

B. Lipids, reagents, and ion channel reconstitution

All lipids were obtained from Avanti Polar Lipids (Alabaster, AL, USA). The cDNA for KcsA was chemically synthesised by Eurofins MWG Operon (Wolverhampton, UK). N-dodecyl-β-D maltopyranoside (DDM) and 5-cyclohexyl-1-pentyl-β-D maltoside (Cymal-5) were

obtained from Anatrace (Maumee, OH, USA) and solvents, α-hemolysin, β-CD, PEG, and TEA were from Sigma-Aldrich (Gillingham, UK).

α-HL was dissolved in 150 mM KCl (10 mM HEPES pH 7.4) buffer at 0.1 mg/ml concentration and 200 μl aliquot stored in a −84 °C freezer. β-CD and TEA solutions were prepared at various concentrations in 1 M KCl (10 mM HEPES pH 7.4) and 150 mM KCl (10 mM MES pH 4.0) buffers, respectively. PEG 1000 and PEG 10 000 were dissolved at the desired concentration in 3 M KCl.

KcsA was cloned into pET28a (Novagen) using NcoI-XhoI restriction sites (NEB). This generated a C-terminal hexa-His tagged protein, together with a two amino acid insertion (Leu, Glu) between the distal end of KcsA and the His-tag. A non-inactivating KcsA channel mutant (E71A) was generated using the QuikChange protocol (Agilent Technologies). The final construct was confirmed by sequencing on both strands. KcsA was expressed, purified, and reconstituted into proteoliposomes as previously described.[15,33] The channel/lipid molar ratio in the proteoliposomes was 1/6000. It is known that the lipid composition modulates KcsA activity,[33] therefore the protein was reconstituted in liposomes and characterized in bilayers of a 1:1 lipid mixture of 1-palmitoyl-2-oleoyl-*sn*-glycero-3-phosphocholine (POPC) and 1-palmitoyl-2-oleoyl-*sn*-glycero-3-phospho-(1′-rac-glycerol) (POPG). Lipids were dissolved in chloroform, mixed in the correct ratio, and dried in a desiccator later dissolved in decane for bilayer formation. Unless otherwise specified for KcsA experiments, the *cis* chamber contained 150 mM KCl, 10 mM HEPES pH 7.4, and the *trans* chamber contained 150 mM KCl, 10 mM MES pH 4.0 solution. Proteoliposomes with reconstituted KcsA channels were added to the *cis* side.

C. Bilayer formation

Bilayer capacitance and ion channel current measurements were made using an ID 526 BLM amplifier with a sampling frequency of 5 kHz and all data is presented without filtering. Potential is measured relative to the *cis* side. Bilayers were formed as follows: the top compartment was filled with buffer (e.g., 1 M KCl, 10 mM HEPES, and pH 7.4) and a slight pressure was applied to fill the hydrophobic microfluidic channel. A 2.5 μl and 8 μl drop of buffer were placed at either end of the microfluidic channel. Bilayers were made from 1,2-diphytanoyl-*sn*-glycero-3-phosphocholine (DPhPC) by painting a 3–5 μl droplet of lipid-decane solution (20 mg/ml) with an acrylic fibre brush. Bilayer formation was monitored by capacitance measurements. Bilayer was usually made at the first attempt; a further attempt gave nearly 100% yield. Note that this manual method of forming bilayers could be automated as described.[9] For α-HL experiments, the protein was added from the *cis* side (top reservoir) with blocker added from the *trans* side (flow channel).

For a 75 μm diameter aperture, the capacitance was typically 15–20 pF, compared with a background capacitance of ∼2–3 pF, which is lower than the typical 10 pF background capacitance of a conventional septum. Taking a typical specific capacitance of a bilayer as 0.45 μF/cm^2,[34] this gives an active bilayer area of approximately 70% of the aperture size. If a smaller bilayer was obtained by painting or if there was no channel insertion within 10 min, the bilayer was broken and reformed to encourage bilayer growth or channel insertion. Without flow, bilayers were stable for 10 days (maximum length of experiment) as presented by authors in an earlier piece of work.[27] With a continuous flow of ∼0.4–0.5 μl/min, the bilayers were stable for several hours.

III. RESULTS AND DISCUSSION

A. Flow rate and bilayer stability

The movement of liquid by surface tension from a small droplet (pumping port) to a large droplet (reservoir port) has been described by Beebe and co-workers.[25,26] Differences in Laplace pressure between the two different sized droplets drives the flow. Whilst the surface area of the droplet on the substrate remains constant, the volumetric flow also remains approximately constant. The contact angle reduces as fluid is depleted from the pump droplet and

replenished in the reservoir droplet. However, at some point the contact area of the droplet begins to reduce, until it finally reaches the area of the port and the flow rate changes.[26] Therefore, a stable flow rate is maintained only when the pump droplet exists in the first phase, i.e., with constant area on the substrate. This means that additional liquid needs to be added to the pump droplet at regular intervals, usually every 3 min to maintain the maximum flow rate. Droplet addition was performed using a pipette, but this procedure could be easily automated with a robotic system. It should be noted that the volume of both droplets can also decrease by evaporation, however the evaporation rate is insignificant compared to the flow rate. We determined the evaporation rate to be 40 ± 5 min for a 2 μl droplet and 80 ± 10 min for an 8 μl droplet at ambient conditions (typically 21 °C and 50% relative humidity).

The volumetric flow rate during pumping is given by

$$\frac{dV}{dt} = \frac{1}{Z}\left[\rho g l - \frac{2\gamma}{R}\right], \tag{1}$$

where Z is the hydrodynamic resistance of the channel, R is the radius of the pumping droplet, ρ is the density of the liquid, g is the gravitational acceleration, l is the height of the reservoir droplet, and γ is the surface free energy of the liquid.[25,26] The flow channel resistance Z is given by

$$Z = \frac{12\mu L}{WH^3\left(1 - 0.63\frac{H}{W}\right)}, \tag{2}$$

where W, H, and L are the width, height, and length of the flow channel and μ is the viscosity of the liquid. For a reservoir droplet height $l = 2$ mm, the flow rate was calculated for three different channel widths, 70 μm, 100 μm, and 200 μm and a range of pump droplet volumes as shown in Fig. 2. The channel height in each case was 55 μm (i.e., one layer of laminate resist) with a channel length of 1.7 cm.

The flow behaviour was also evaluated experimentally using tracer particles (100 nm fluorescent beads). Two droplets of 150 mM KCl were placed on the reservoir (8 μl) and pump (2.5 μl) ports, and after 3 min an additional 1.25 μl droplet containing fluorescent beads (0.002% w/v) was placed on top of the depleted pump droplet. The fluorescence intensity was measured at the aperture in the absence of a bilayer. Further 1.25 μl droplets of buffer (without beads) were added every 3 min to the pump drop. Addition of the droplet with beads produced an immediate spike in the fluorescence. This intensity decreased exponentially as the channel was washed with subsequent buffer-only droplets, as shown in Fig. 3. After 15 min of flowing buffer solution, the fluorescence intensity reduced to <4% of its peak value. With the employed droplet sizes and channel dimensions (55 μm high and 100 μm wide), the estimated flow rate was ~0.42 μl/min, which is consistent with the prediction of Fig. 2. For a channel length of

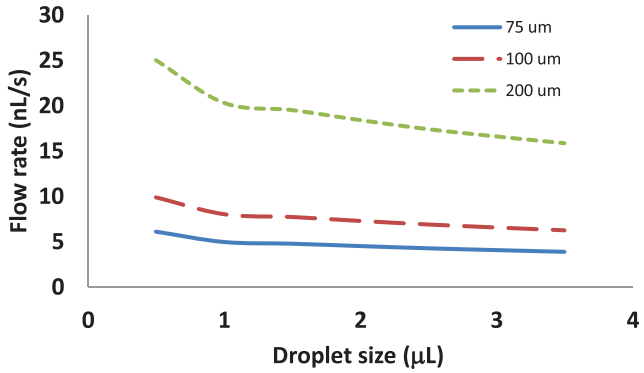

FIG. 2. Variation in calculated flow rate vs pump droplet volume. The flow channel is 55 μm high and 1.7 cm long. The theoretical flow rate as a function of pump droplet volume is shown for three different channel widths.

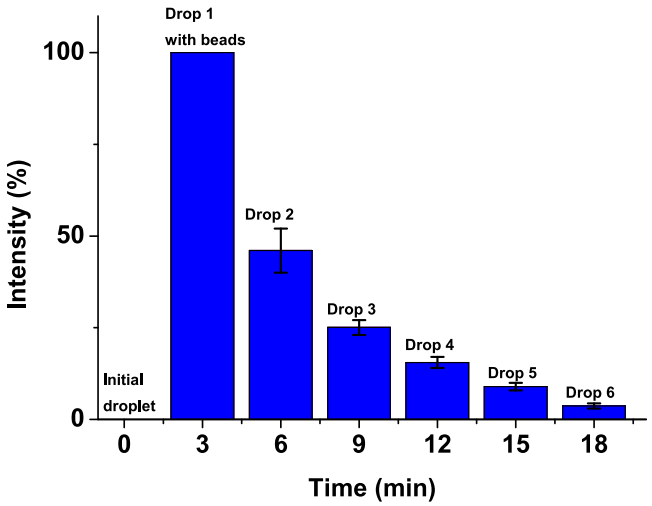

FIG. 3. Average fluorescence intensity of tracer beads vs time at a constant flow rate of ∼0.42 μl/min. The initial pumping droplet size was 2.5 μl and a 1.25 μl drop was added at the pump port every 3 min. The channel width, height, and length were 100 μm, 50 μm, and 1.7 cm, respectively. Error bars are one S.E.M. for three repeat experiments.

1.7 cm, the entire volume of the flow channel is 100 nl, much smaller than the volume of droplet 17 μl (Ref. 24) and bottom compartment 30 μl.[23] Therefore, the device would require significantly smaller amount of buffer (∼10 μl) to clean the flow channel compare to hundreds of microlitres in reported work.[23,24]

The flow rate was also measured in the presence of a bilayer, whilst simultaneously recording the capacitance (aperture of 75 μm, flow channel 70 μm wide, 55 μm high, and 1.5 cm long). At a flow rate of 0.35 μl/s, the sample reaches the bilayer within 10 s (see supplementary material video S1 (Ref. 30)).

To quantify bilayer rupture probability, bilayers were measured for various sizes of droplets determined from observations with an optical microscope. Droplet sizes were estimated with trigonometric function for a spherical cap.[26] After bilayer formation from DPhPC-decane solution, a droplet was placed at the pumping port and bilayer stability was monitored by capacitance measurements. The number of bilayers tested was >10. Fig. 4 shows the bilayer rupture probability versus pumping port droplet size. For a droplet of 0.5 μl (flow rate ∼0.6 μl/s), the probability of bilayer breakage was around 50%. For a droplet size of 1 μl, the probability reduced to 25%, and for a 1.5 μl droplet it was less than 10% (Fig. 4). For the channel dimensions used in this work (100 μm channel width) an initial droplet size of 2.5 μl was found to be optimum, with an addition of a further 1–1.25 μl every 3–4 min to maintain a stable flow rate of ∼0.4 μl/min without bilayer rupture.

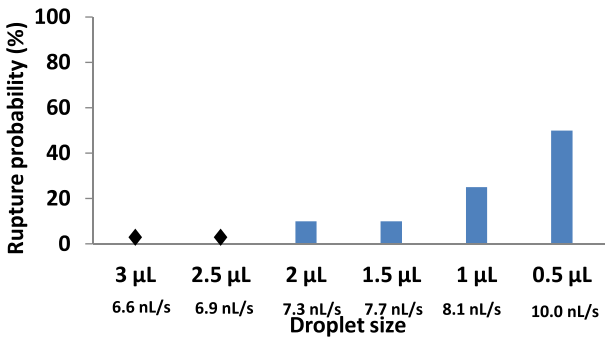

FIG. 4. Rupture probability for a bilayer with different sized droplets at the pumping port. The channel width is 100 μm, the channel width is 55 μm, and the channel length is 1.7 cm. For each pumping droplet size, the number of measured bilayers was >10. For droplet volumes > 2 μl and flow rates of approximately 7 nl/s, the bilayers were stable for hours.

Previous authors have demonstrated that bilayers can be perfused at higher flow rates. Shao *et al.*[21] used a flow system to measure the response of ion channels to inhibitors. With channel dimensions of 460 × 120 μm, bilayers were stable up to a steady state flow rate of 2.5 μl/min (and up to 20 μl/min for a short duration). Considering that the cross section of the channel in our device is 10 times smaller, this is a similar scaled flow rate. The time required for compounds to reach the bilayer can also be calculated[21] where a switching time is defined as the time required for the concentration of solute to change from 5% to 95%. At our maximum flow rate of 0.4 μl/min, the switching time (τ) for the TEA blocker ($D = 5 \times 10^{-10}$ m^2/s)[35] is ~4 s. This is shorter than reported for small ions such as La^{2+} at much higher flow rates of 10 μl/min,[21] highlighting the advantage of smaller microfluidic channels.

B. Ion channel measurements

Dose-dependent blocking of α-hemolysin with β-CD is shown in Fig. 5. After bilayer formation, α-hemolysin pores were incorporated by addition of protein to the *cis* side reservoir. Spontaneous insertion of one or two channels occurred after 1–2 min, as shown in Fig. 5(a). Transient blocking was observed within a few seconds of adding β-CD to the *trans* side flow channel of the bilayer via a single droplet (Fig. 5(b)). The frequency of blocking events increased with β-CD concentration (Figs. 5(b) and 5(c)), consistent with published data.[28] After flushing with buffer-only solution, very few events α-hemolysin blocking events were observed (Fig. 5(d)), demonstrating efficient perfusion of the β-CD blocker compound. The blocking frequency was quantified over discrete time windows of 10 s. An event was scored if the current dropped to a value of 4σ below the open pore currents,[36] where the standard deviation σ is the peak-to-peak noise of the baseline current, which was ~2 pA (Figs. 5(a) and 5(d)). The blocking frequency increased with β-CD concentration as shown in Table I, consistent with published

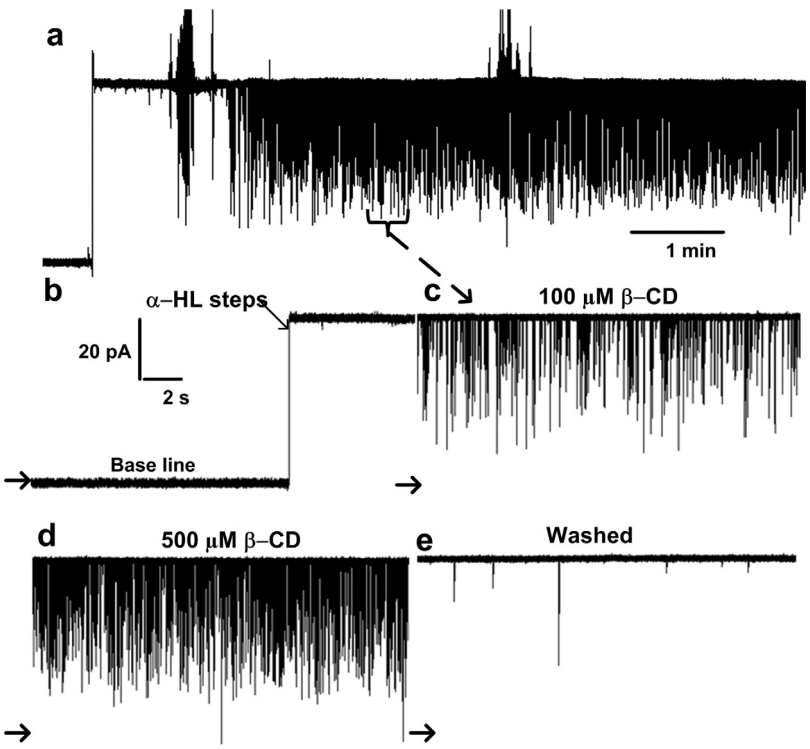

FIG. 5. Flow channel perfusion of β-CD. (a) Current trace of α-hemolysin in the presence of the β-CD blocker, in 1 M KCl buffer. Current traces of a shorter time scale show (b) bilayer insertion of a single α-hemolysin channel, (b) and (c) transient channel blocking events induced by (c) 100 μM β-CD and (d) 500 μM β-CD, and (e) the α-hemolysin current without significant β-CD blocking after rinsing the flow channel with buffer-only solution. The applied potential was +50 mV and the sampling frequency was 5 kHz, with no additional filtering.

TABLE I. Frequency of α-hemolysin blocking events for the flow channel sequence buffer solution–100 μM β-CD–500 μM β-CD–buffer solution. Data are taken from 10 s bins. An event is scored positive when the current is 4σ below the open pore current, where σ is approximately 2 pA. The error bar is the standard deviation from three separate experiments.

β-CD concentration (μM)	Number of events/s (mean)	Standard deviation (±)
0 (at start)	0	0
100	10.24	1.46
500	38.88	2.42
0 (after clean)	0.96	0.2

data.[28,37] Bilayers were stable with no breakage during all these experiments, which could continue for several hours.

Transient blocking of α-hemolysin with two different PEG molecules is shown in Fig. 6. A buffer solution of 3 M KCl was used to maximize polymer-pore attraction.[38] The α-hemolysin protein was added to the *cis* compartment. PEG solutions (0.5 mg/ml (Ref. 39)) were introduced via the *trans* (bottom) channel (PEG 1000, followed by clean buffer, then PEG 10 000). Spontaneous blocking events were observed with PEG 1000 as shown in Fig. 6(a) (see supplementary material Fig. S2 for a long time trace[30]); residual currents were around 14%–18% of the open pore current, as previously observed.[38] Ion channel exposure to the higher molecular-weight PEG (PEG 10000) further reduced the residual current to ∼4%–6% of the open pore current (Fig. 6(b)), confirming that the amplitude of the blockage varies with the molecular weight of the PEG.[38] Histograms of blocking events are shown in Figs. 6(c) and 6(d) for PEG

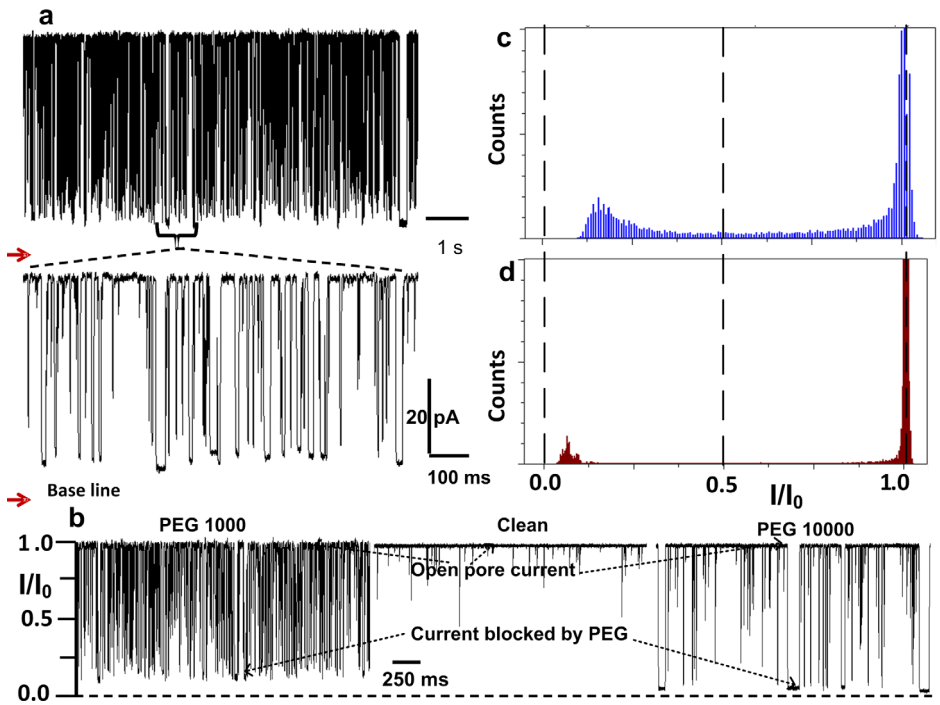

FIG. 6. Blocking of α-hemolysin channels by PEG in 3 M KCl solution at 20 mV. (a) Single blocking events due to PEG 1000 shown for two different time scales. (b) Normalised current trace showing blocking of a single α-HL pore in the presence of PEG 1000, followed by clean buffer, then after the introduction of PEG 10 000. The open pore current and the current after blocking by PEG are highlighted by the arrows. Current histograms of blocking events are shown in (c) for PEG 1000 and (d) for PEG 10 000. For each histogram, a 5 s duration trace was chosen, with bin width 0.001 pA (data processed with Clampfit software). Sampling frequency for all recordings was 5 kHz, with no additional filtering. I_0 is the open pore current and I is the current with PEG blocker.

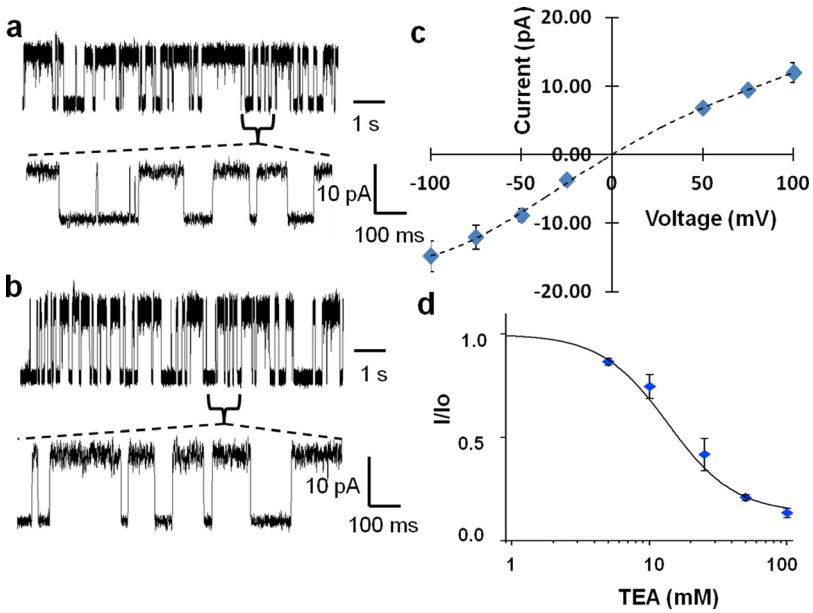

FIG. 7. Electrophysiological measurements with KcsA-E71A ion channel, incorporated in the on-chip aperture-suspended bilayer by vesicle fusion. The *cis* reservoir contains 150 mM KCl, 10 mM HEPES pH 7.4 buffer, and the *trans* flow channel contains 150 mM KCl, 10 mM MES pH 4.0 buffer. Current traces recorded at (a) +50 mV and (b) +75 mV display single-channel KcsA gating events. (c) Current-voltage relationship for KcsA single-channel conductance. Error bars are standard deviations obtained from four separate bilayers. (d) Normalised ion-channel conductance for different TEA^+ blocker concentrations in the *trans* flow channel. Fitting to the Hill equation gives an IC_{50} value of 13.6 mM. The bilayer aperture for (a)–(c) was 60 μm and for (d) 75 μm.

1000 and PEG 10 000, respectively. This method allows the length of an unknown PEG molecule to be rapidly correlated with current block levels and bilayer current histograms.

Finally, to demonstrate ion channel incorporation by vesicle fusion and asymmetric electrophysiology buffer experiments, current traces were recorded for the pH-gated ion channel KcsA.[16] Following formation of stable bilayers, ~2.5 μl of proteoliposome dispersion was added to the *cis* chamber. Only those channels that insert with the intracellular side facing the *trans* (pH 4.0) chamber will be active; channels inserting with the intracellular side facing the *cis* (pH 7.4) chamber will be functionally silent.[16,17,32] Characteristically, KcsA displays long-lived "quiet" or closed intervals and exhibits low open probabilities,[16] hence we used the non-inactivating KcsA mutant (E71A) where the long closures have been abolished and the open probability is >90%.[40] Single-channel KcsA-E71A traces in symmetrical 150 mM KCl solutions were obtained, demonstrating proteoliposome fusion with the aperture-suspended bilayer and bilayer incorporation of a non-toxin ion channel. Selected traces and a current voltage relationship derived from a larger data set are shown in Fig. 7 and are in agreement with published results.[40,41]

The flow channel was subsequently utilized to expose bilayer-incorporated KcsA-E71A to a sequence of solutions, of increasing concentration, of the potassium channel blocker tetraethylammonium (TEA^+).[17,40] Concentration-dependent modulation of KcsA activity was observed, summarised in Fig. 7(d), and analysis gave an IC_{50} value of 13.6 mM, correlating with literature.[40] Significantly, the modulation of E71A-KcsA activity by TEA was characterized using only 100 μg of compound (15 μl volume) in 30 min.

IV. CONCLUSION

We have developed a compact, simple, and scalable planar bilayer chip technology based on micro-cavities with integrated electrodes and microfluidic passive flow. The bilayer chips are simple to manufacture from dry film resist and the passive pumping method eliminates the need for unwieldy syringe pumps and tubes with associated material wastage.[7,8,19] The

perfusion system was demonstrated using three model systems: (1) α-HL insertion on the *cis* side, with β-CD blocker introduced to and flushed out of the *trans* flow channel, (2) α-HL transient blocking with different molecular weight PEGs via the flow channel, and (3) KcsA-E71A proteoliposome fusion from the *cis* compartment, and concentration-dependent TEA^+ blocking of the bilayer-incorporated KcsA mutant from the flow channel. Compared with traditional bilayer electrophysiology systems,[28,29] which use large-volume cups and an aperture in a Teflon septum, both the bilayer and the shunt capacitance are considerably reduced, resulting in higher quality electrical recordings (see supplementary material Fig. S3 (Ref. 30)). Although our system does not require continuous pumping of liquids with pumps and the associated tubing, nevertheless discrete μl droplets must be added to the device to maintain a constant flow. At the flow rates described here, this amounts to a droplet every few minutes, a process which could be easily automated with the use of a micro-pipetting robot system. We believe that this method provides a simple and efficient way of delivering compounds to ion channels, transporters, or nanopores incorporated in phospholipid bilayers. In contrast to conventional bilayer technology, the method provides a novel means of drug screening against ion channels using very small volumes of compound solutions (10–15 μl) compared to the state of the art,[19–23] significantly reducing the cost per screen. The chips are easy to manufacture on a wafer and could be reused if necessary. The use of dry film resists for chip manufacture gives an aperture with low shunt capacitance and a microfluidic channel of the appropriate dimensions in a single fabrication step. The bilayers are mechanically very stable enabling solution exchange without rupturing the bilayer up to 7 nl/s. Although we used passive droplet pumping for these chips, they could equally be interface with conventional microfluidic pumping systems if so desired. The system is ideal for parallel electrophysiology assays and provides a novel tool for drug screening, where a range of target compounds could be quickly titrated against different membrane proteins.

ACKNOWLEDGMENTS

This work was funded by the Engineering and Physical Sciences Research Council (EP/H044795/1 to H.M. and MdP and EP/H043888/1 to B.A.W.). The authors would like to thank Yan Zhao for help with the confocal microscopy.

[1]B. Hille, *Ion Channels of Excitable Membranes*, 3rd ed. (Sinauer Associates, Sunderland, 2001).
[2]M. L. Garcia, Nature **430**, 153 (2004).
[3]D. D. Duan and T.-H. Ma, Acta Pharmacol. Sin. **32**, 673 (2011).
[4]D. C. Camerino, D. Tricarico, and J.-F. Desaphy, Neurotherapeutics **4**, 184 (2007).
[5]P. Kongsuphol, K. B. Fang, and Z. Ding, Sens. Actuators, B **185**, 530 (2013).
[6]J. Dunlop, M. Bowlby, R. Peri, D. Vasilyev, and R. Arias, Nat. Rev. Drug Discov. **7**, 358 (2008).
[7]R. Kawano *et al.*, Sci. Rep. **3**, 1995 (2013).
[8]M. Zagnoni, M. E. Sandison, and H. Morgan, Biosens. Bioelectron. **24**, 1235 (2009).
[9]G. Baaken, M. Sondermann, C. Schlemmer, J. Ruhe, and J. C. Behrends, Lab Chip **8**, 938 (2008).
[10]S. D. Ogier *et al.*, Proc. SPIE **4235**, 452 (2001).
[11]R. Kawano, T. Osaki, H. Sasaki, and S. Takeuchi, Small **6**, 2100–2104 (2010).
[12]J. K. Rosenstein, M. Wanunu, C. A. Merchant, M. Drndic, and K. Shepard, Nat. Methods **9**, 487 (2012).
[13]B. Le Pioufle, H. Suzuki, K. V. Tabata, H. Noji, and S. Takeuchi, Anal. Chem. **80**, 328 (2008).
[14]A. Hirano-Iwata, K. Aoto, A. Oshima, T. Taira, R.-t. Yamaguchi, Y. Kimura, and M. Niwano, Langmuir **26**, 1949 (2010).
[15]S. Kalsi, A. M. Powl, B. A. Wallace, H. Morgan, and M. R. R. de Planque, Biophys. J. **106**, 1650 (2014).
[16]M. LeMasurier, L. Heginbotham, and C. Miller, J. Gen. Physiol. **118**, 303 (2001).
[17]E. Kutluay, B. Roux, and L. Heginbotham, Biophys. J. **88**, 1018 (2005).
[18]B. Hornblower *et al.*, Nat. Methods **4**, 315 (2007).
[19]V. C. Stimberg, J. G. Bomer, I. van Uitert, A. van den Berg, and S. Le Gac, Small **9**, 1076 (2013).
[20]Y. Tsuji, R. Kawano, T. Osaki, K. Kamiya, N. Miki, and S. Takeuchi, Lab Chip **13**, 1476 (2013).
[21]C. Shao, B. Sun, M. Colombini, and D. L. De Voe, Ann. Biomed. Eng. **39**, 2242 (2011).
[22]S. A. Portonovo and J. Schmidt, Biomed. Microdevices **14**, 187 (2012).
[23]S. A. Acharya, A. Portman, C. S. Salzer, and J. Schmidt, Sci. Rep. **3**, 3139 (2013).
[24]M. Zagnoni, M. E. Sandison, P. Marius, and H. Morgan, Anal. Bioanal. Chem. **393**, 1601 (2009).
[25]G. M. Walker and D. J. Beebe, Lab Chip **2**, 131 (2002).
[26]E. Bertheir and D. J. Beebe, Lab Chip **7**, 1475 (2007).
[27]S. C. Saha, F. Thei, M. R. R. de Planque, and H. Morgan, Sens. Actuators, B **199**, 76 (2014).

[28]F. Thei, M. Rossi, M. Bennati, M. Crescentini, F. Lodesani, H. Morgan, and M. Tartagni, IEEE Trans. Nanotechnol. **9**, 295 (2010).
[29]G. Maglia, A. J. Heron, D. Stoddart, D. Japrung, and H. Bayley, Methods Enzymol. **475**, 591 (2010).
[30]See supplementary material at http://dx.doi.org/10.1063/1.4905313 for fluid flow without bilayer rupture, the process flow for fabrication of the chip, a long time trace for PEG 1000, a comparison of an electrical recording with the flow channel chip, and a traditional bilayer setup.
[31]B. J. Polk *et al*., Sens. Actuators, B **114**, 239–247 (2006).
[32]N. Wangler *et al*., J. Micromech. Microeng. **21**, 095009 (2011).
[33]P. Marius, M. Zagnoni, M. E. Sandison, J. M. East, H. Morgan, and A. G. Lee, Biophys. J. **94**, 1689 (2008).
[34]M. Montal and P. Mueller, Proc. Natl. Acad. Sci. U.S.A. **69**, 3561 (1972).
[35]E. Koppenhofer and W. Vogel, Pflugers Arch. **313**, 361 (1969).
[36]L. P. Hromada, B. J. Nablo, J. J. Kasianowicz, M. A. Gaitan, and D. L. DeVoe, Lab Chip **8**, 602 (2008).
[37]T. Osaki, H. Suzuki, B. Le Pioufle, and S. Takeuchi, Anal. Chem. **81**, 9866 (2009).
[38]O. V. Krasilnikov, C. G. Rodrigues, and S. M. Bezrukov, Phys. Rev. Lett. **97**, 018301 (2006).
[39]G. Baaken, N. Ankri, A.-K. Schuler, J. Ruhe, and J. C. Behrends, ACS Nano **5**, 8080 (2011).
[40]E. Vales and M. Raja, J. Membr. Biol. **234**, 1 (2010).
[41]S. Banerjee and C. M. Nimigean, J. Gen. Physiol. **137**, 217 (2011).